# TRANSPORT PROPERTIES FOR AN INTERMEDIATE VALENCE MODEL OF $Tl_2Mn_2O_7$.

M.E. Foglio and G.E. Barberis
*Instituto de Física "Gleb Wataghin", UNICAMP,13083-970, Campinas, São Paulo, Brazil.*
(Dated: February 2, 2008)

The appearance of colossal magneto resistance (CM) in $Tl_2Mn_2O_7$ has stimulated many recent studies of the pyrochlore family of compounds $A_2B_2O_7$. The double exchange (DE) model of Zener does not describe the CM in $Tl_2Mn_2O_7$, because its metallic conductivity cannot be explained by doping. Here we employ Hubbard operators to reformulate the intermediate valence model used by Ventura and Alascio to describe the electronic structure and transport properties of this compound (*Phys.Rev.* **B**56, 14533 (1997)). Following Foglio and Figueira (*Phys.Rev.* **B**62, 7882, (2000)) we use approximate one-electron Green's Functions (GF) to calculate the thermopower and the static and dynamic conductivity of $Tl_2Mn_2O_7$ for several magnetic fields. A qualitative agreement was obtained with the experimental measurements of those properties. Although the agreement is far from perfect, these quantities are fairly well described by the same set of system parameters.

PACS numbers: 75.70.Pa.

## I. INTRODUCTION

The $A_2B_2O_7$ pyrochlore family of compounds has been the object of many recent studies, principally because of the appearance of colossal magneto resistance (CM) in the $Tl_2Mn_2O_7$ compound. This material was reported as ferromagnetic, metallic and with enormous negative magneto resistance in the region of temperatures corresponding to the ferromagnetic transition (Tc $\sim$ 121 K). The principal interest created for this material is that the double exchange (DE) Zener model does not explain the CM in this material. Experimental studies show that, when compared with other $A_2Mn_2O_7$ compounds, the Tl one is unique. It has a very high Tc, a property shared with the In pyrochlore, but it is the only compound of the series that presents metallic conductivity, which cannot be explained by doping because it is present in the stoichiometric compound. Several recent band calculations[1,2,3] show that the material is expected to be almost half metallic at low temperatures, that is, the conductivity is driven within only one of the spin directions. This property is the same for the DE perovskites, but in that case the conductivity and the ferromagnetism appear only with doping.

The whole family of Mn pyrochlores shows ferromagnetism,[4] and their bands present similarities, with a band gap reducing its value from Y to Tl, where the compound is slightly metallic with very different conductivity for the both spin directions. The ferromagnetism in the Mn pyrochlore compounds is explained by the Kanamori-Goodenough rules, as the result of superexchange through the O ligands. However, the Curie temperatures do not scale with the bond angles, which seems to indicate a different mechanism for the In and Tl compounds[4](The calculated values of the exchange parameter $J$ for the Tl, In, and Y compounds are respectively 0.11 K, 2.52 K, and 1.1K, but their corresponding measured Tc's are 124 K, 129 K and 16 K).

The experimental paper published by Raju et al.[5] tries to explain the ferromagnetism of the Tl compound through DE, but several evidences proved afterwards that the origin of ferromagnetism is only superexchange.

A small number of carriers, of the order found in doped semiconductors [$\sim 10^{19} cm^{-3}$], was found in the Tl compound by measuring Hall effect[6]. Several authors obtain a large enhancement of the magnetoresistance[2,7] by doping the Tl sites with In and Sc, or the Mn sites with Ru. The behavior of the resistivity is sample dependent[6,8] at high T, which created a controversy about the compound behavior in this region of temperatures.

Imai et al[9] present the more complete set of measurements of Hall effect and magneto-thermopower. They measured the anomalous Hall coefficient at low (below Tc) and high temperatures, and they found it small in both cases. Following Singh[1] they assume a very simple quasi spherical Fermi surface and fit the thermopower to the effective mass model.

The pressure reduces the value of Tc for all the Mn pyrochlores.[10] Nuñez- Regueiro and Lacroix[11] developed a theory for this effect that gives good agreement with the experimental results, confirming that the ferromagnetism is due to superexchange.

Ventura and Alascio[12] used an intermediate valence (IV) model for the Tl, and they could explain both the conductivity and the CM of the pure Tl compound. Here we refine their calculations, using the same IV model, but employing Hubbard X operators.[13] We calculate both the static and dynamic conductivity and a qualitative agreement with the measured quantities was obtained[14,15], without having to assume an O deficiency. This agrees with the result of the published band studies[1,2,3]. Following Schweitzer and Czycholl[16] we calculate the thermopower and magnetothermopower, and our results agree with the experiments.[9]

In Section II we reformulate the model of Ventura and Alascio, employing the Hubbard operators. We discuss the approximate GF that we employ in the calculation,

and give the formulae to calculate the resistivity, optical conductivity and thermopower. In Section III we discuss the parameters we shall use, and calculate the transport properties and in Section IV we present our conclussions. Finally, we give an Appendix with the atomic states employed to calculate the GF.

## II. THE MODEL WITH $X$-OPERATORS

The model employed[12] is a lattice of local states hybridized with a conduction band. Each local state has two magnetic configurations with spin $S = 1/2$ and $S = 1$ respectively, that are hybridized with the conduction electrons. The local state with $S_z = 0$ of the $S = 1$ configuration is discarded, so that we have two independent systems with spin up and spin down respectively because the hybridization conserves the spin direction. Each local site $j$ has then two states $|j, \sigma\rangle$ with $S = \frac{1}{2}, \sigma = \pm\frac{1}{2}$ and two states $|j, s\rangle$ with $S = 1, s = \pm 1$, and their respective energies are $E_\sigma$ and $E_s$.

We can give assume arbitrary properties and energies for the relevant localized states of this model, and it is then convenient to describe them employing Hubbard operators $X_{j;a,b} = |j, a\rangle \langle j, b|$, which transform the state $|j, b\rangle$ into the state $|j, a\rangle$, i.e. $X_{j,ab} |j, b\rangle = |j, a\rangle$. These operators do not satisfy Wick's theorem, and their product rules at the same site have to be used instead:

$$X_{j,ab}\ X_{j,cd} = \delta_{b,c}\ X_{j,ad}. \tag{1}$$

When the operators are at different sites we chose properties equivalent to those of the usual Fermi or Bose: we say that $X_{j,ab}$ is of the "Fermi type" ("Bose type") when the number of electrons in the two states $|\ j, a\rangle$ and $|\ j, b\rangle$ differ by an odd (even) number. For $j \neq j'$ we then use $\{X_{j,ab}, X_{j',cd}\} = 0$ when the two operators are of the "Fermi type" and $[X_{j,ab}, X_{j',cd}] = 0$ when at least one is of the "Bose type" (as usual[19] $[a, b] = ab - ba$ and $\{a, b\} = ab + ba$).

We write the model's Hamiltonian employing :

$$H = \sum_{j,\sigma}\ E_\sigma\ X_{j;\sigma\sigma} + \sum_{j,s} E_s X_{j;ss} + \sum_{\mathbf{k},\sigma} E_{\mathbf{k},\sigma} c^\dagger_{\mathbf{k},\sigma} c_{\mathbf{k},\sigma} + \\ + \sum_{j,\mathbf{k},\sigma} \left( V_{j,\mathbf{k},\sigma} X^\dagger_{j;\sigma,s=2\sigma}\ c_{\mathbf{k},\sigma} + V^*_{j,\mathbf{k},\sigma}\ c^\dagger_{\mathbf{k},\sigma} X_{j;\sigma,s=2\sigma} \right) \tag{2}$$

where we denote the Hubbard operators $X_{j;\pm\frac{1}{2},\pm 1}$ with $X_{j;\sigma,s=2\sigma}$ (note that $X_{j;b,a} = X^\dagger_{j;a,b}$). The $c^\dagger_{\mathbf{k},\sigma}$ and $c_{\mathbf{k},\sigma}$ are the creation and destruction operators of a conduction electron with energies $E_{\mathbf{k},\sigma}$, wave vector $\mathbf{k}$, and spin component $\sigma\hbar/2$, where $\sigma = \pm 1$, and the hybridization constant is

$$V_{j,\mathbf{k},\sigma} = \left(1/\sqrt{N_s}\right) V(\mathbf{k}) \exp\left(i\mathbf{k}.\mathbf{R_j}\right), \tag{3}$$

where $V(\mathbf{k})$ is independent of $\mathbf{k}$ when the mixing is purely local and $N_s$ is the number of sites.

The cumulant expansion was extended by Hubbard[20] to study a quantum problem with fermions, and he derived a diagrammatic expansion involving unrestricted lattice sums of connected diagrams that satisfies a linked cluster theorem. The extension of this technique to the Anderson lattice[21] is sufficiently general to treat the model described by Eq. (2), and is the basis of the present treatment. One has to use the Grand Canonical Ensemble of electrons, and it is then convenient to introduce

$$\mathcal{H} = H - \mu \left\{ \sum_{\vec{k},\sigma} C^\dagger_{\vec{k},\sigma} C_{\vec{k},\sigma} + \sum_{ja} \nu_a X_{j,aa} \right\} \quad , \tag{4}$$

where $\mu$ is the chemical potential and $\nu_a$ is the number of electrons in the state $|j, a\rangle$, and without any restriction for the treatment we shall use $\nu_{\pm\frac{1}{2}} = 0$ and $\nu_{\pm 1} = 1$. It is also convenient to introduce

$$\varepsilon_{j,a} = E_{j,a} - \mu\ \nu_a \tag{5}$$

$$\varepsilon_{\mathbf{k}\sigma} = E_{\mathbf{k}\sigma} - \mu \quad , \tag{6}$$

because these are the forms that consistently appear in the calculations.

The last term in Eq. (2) will be considered as the perturbation, and the exact and unperturbed averages of any operator $A$ shall be respectively denoted by $< A >_{\mathcal{H}}$ and $< A >$.

### A. The Approximate Green's functions

As in the Anderson lattice[13] with $U \to \infty$ one can introduce one-particle Green's functions (GFs) of local electrons

$$\left\langle \left( X_{j;\sigma,s=2\sigma}(\tau)\ X^\dagger_{j;\sigma,s=2\sigma}(\tau') \right)_+ \right\rangle_{\mathcal{H}} \quad , \tag{7}$$

as well as GFs for the c-electrons $\left\langle \left( C_{k\sigma}(\tau)\ C^\dagger_{k'\sigma}(\tau') \right)_+ \right\rangle_{\mathcal{H}}$ and "crossed" GFs of the type $\left\langle \left( X_{j;\sigma,s=2\sigma}(\tau)\ C^\dagger_{k'\sigma}(\tau') \right)_+ \right\rangle_{\mathcal{H}}$, all of them defined in the intervals $0 \leq \tau, \tau' \leq \beta \equiv 1/T$. It is possible to associate a Fourier series to these GFs because of their boundary condition in this variable,[21] and the coefficients $\left\langle \left( X_{j;\sigma,s=2\sigma}(\omega_\nu)\ X^\dagger_{j;\sigma,s=2\sigma}(\omega_{\nu'}) \right)_+ \right\rangle_{\mathcal{H}+}$ correspond to the Matsubara frequencies $\omega_\nu = \pi\nu/\beta$ (where $\nu$ are all the positive and negative odd integer numbers). One can also transform the GF to reciprocal space,[21] and because of the invariance against time and lattice translations

$$\left\langle \left( X_{j;\sigma,s=2\sigma}(\omega_\nu)\ X^\dagger_{j;\sigma,s=2\sigma}(\omega_{\nu'}) \right)_+ \right\rangle_{\mathcal{H}} = \\ G_{ff,\sigma}(\mathbf{k}, \omega_\nu)\ \delta_{\mathbf{k}',\mathbf{k}}\ \delta_{\nu+\nu',0}. \tag{8}$$

Transforming the eigenstates of the c-electrons to the Wannier representation, one also obtains the equivalent relations for $G_{cc,\sigma}(\mathbf{k},\omega_\nu)$ and $G_{fc,\sigma}(\mathbf{k},\omega_\nu)$. Considering that the coefficients of the $\tau$ Fourier series for each $\mathbf{k}$ are the values of a function of the complex variable $z=\omega+iy$ at the points $z_\nu = i\,\omega_\nu$, it is possible to make the analytic continuation to the upper and lower half-planes of $z$ in the usual way,[25] obtaining, e.g. from the $G_{ff,\sigma}(\mathbf{k},\omega_\nu)$, a function $G_{ff,\sigma}(\mathbf{k},z)$ which is minus the Fourier transform of the double time GF.[26]

The one-electron GF of ordinary Fermions or Bosons can be expressed as a sum of infinite "proper" (or irreducible) diagrams,[19] and a similar result was obtained for the Hubbard model employing the cumulant expansion[22] with the hopping as perturbation. In the cumulant expansion of the Anderson lattice[21] we employed the hybridization rather than the hopping as a perturbation, and the exact solution of the conduction electrons problem in the absence of hybridization was included in the zeroth order Hamiltonian. It was then necessary to extend Metzner's derivation[22] to the Anderson lattice, and the same type of results he derived were also obtained for the Anderson lattice. As with the Feynmann diagrams, one can rearrange all those that contribute to the exact $G_{ff,\sigma}(\mathbf{k},\omega_\nu)$ by defining an effective cumulant $M^{eff}_{2,\sigma}(\mathbf{k},\omega_\nu)$, that is given by all the diagrams of $G_{ff,\sigma}(\mathbf{k},\omega_\nu)$ that can not be separated by cutting a single edge (usually called "proper" or "irreducible" diagrams). The exact one-particle GFs of the Anderson lattice[13,18] were then obtained by introducing the $M^{eff}_{2,\sigma}(\mathbf{k},\omega_\nu)$ in the cumulant expansion, and the model employed in those works was sufficiently general, so that their results could be easily extended to the Hamiltonian in Eq. (2) in the present work.

By analytical continuation one then obtains the formal expressions of the exact one-particle GFs of our model:

$$G_{ff,\sigma}(\mathbf{k},z) = \frac{M^{eff}_{2,\sigma}(\mathbf{k},z)}{1- \mid V(\mathbf{k}) \mid^2 G^{o}_{c,\sigma}(\mathbf{k},z)\; M^{eff}_{2,\sigma}(\mathbf{k},z)}, \quad (9)$$

and

$$G_{cc,\sigma}(\mathbf{k},z) = \frac{-1}{z-\varepsilon_{\mathbf{k}\sigma} + \mid V(\mathbf{k}) \mid^2 M^{eff}_{2,\sigma}(\mathbf{k},z)}, \quad (10)$$

where $G^{o}_{c,\sigma}(\mathbf{k},z) = -1/(z-\varepsilon_{\mathbf{k}\sigma})$ is the free c-electron propagator.

The calculation of $M^{eff}_{2,\sigma}(\mathbf{k},\omega_\nu)$ is as difficult as that of $G_{ff,\sigma}(\mathbf{k},\omega_\nu)$, and it is then convenient to use an approximation: we shall replace $M^{eff}_{2,\sigma}(\mathbf{k},\omega_\nu)$ by the corresponding quantity $M^{at}_{2,\sigma}(\omega_\nu)$ of an exactly soluble Hamiltonian, namely the one describing the atomic limit of the same model. Although the hopping is neglected in this system, described by the Hamiltonian of Eqs. (2) with $E_{\mathbf{k},\sigma} = E_{0,\sigma}$ and with a local hybridization $V(\mathbf{k}) = V$, the $M^{at}_{2,\sigma}(\omega_\nu)$ implicitly contains all the higher order cumulants that appear in the exact quantity. In the case of the Anderson lattice, the atomic limit contains the basic physics of the formation of the singlet ground state and of the appearance of the Kondo peak,[23,24] and we expect that it would provide an adequate description of the present model. Because of its atomic character, the approximate effective cumulant $M^{at}_{2,\sigma}(\omega_\nu)$ thus obtained is independent of $\mathbf{k}$, and can be calculated exactly as discussed below.

With the approximations introduced above and employing the Wannier representation for the $c$-electron operators the whole system becomes a collection of local systems, described by a Hamiltonian $\sum_j H_j$, where $H_j$ is the local Hamiltonian at site $j$. This $H_j$ can be solved exactly:

$$H_j \mid j,\nu,r\rangle = E_{\nu,r} \mid j,\nu,r\rangle, \quad (11)$$

where $\mid j,\nu,r\rangle$ is the eigenstate at site $j$ with energy $E_{\nu,r}$, that is characterized by $r$ and its number $\nu$ of electrons. Because of the translational invariance we shall drop the site index $j$ when it is not necessary, and we shall also use the quantities $\varepsilon_{\nu,r} = E_{\nu,r} - \nu\mu$, more adequate for the $\mathcal{H}$ in Eq. (4) than the $E_{\nu,r}$ (for convenience we use $\nu_{\pm\frac{1}{2}} = 0$ and $\nu_{\pm 1} = 1$). In the Appendix we give in Table I the properties of the $\mid \nu,r\rangle$ states: the number $r$ that identifies the state, the $z$ component of spin $S_z$ and the quantities $\varepsilon_{\nu,r} = E_{\nu,r} - \nu\mu$ .

It is now straightforward to express the Fourier transform $G^{at}_{ff,\sigma}(\omega_s)$ of the f-electron GF in the atomic limit

$$G^{at}_{ff,\sigma}(\omega_s) = -e^{\beta\Omega} \sum_{\nu,r,r'} \frac{\exp(-\beta\varepsilon_{\nu,r}) + \exp(-\beta\varepsilon_{\nu-1,r'})}{i\omega_s + \varepsilon_{\nu-1,r'} - \varepsilon_{\nu,r}} \times \mid \langle \nu-1,r' \mid X_{\sigma,s=2\sigma} \mid \nu,r\rangle \mid^2, \quad (12)$$

where $\Omega = -kT \ln \sum \exp(-\beta\epsilon_{\nu,r})$ is the grand canonical potential.[28] The equivalent equations for the c-electrons are obtained by just replacing $\mid \langle \nu-1,r' \mid X_{\sigma,s=2\sigma} \mid \nu,r\rangle \mid^2$ in Eq. (12) by $\mid \langle \nu-1,r' \mid C_{j,\sigma} \mid \nu,r\rangle \mid^2$.

The f-electron GF can be written in the form

$$G^{at}_{ff,\sigma}(\omega_s) = -\exp(\beta\Omega) \sum_{j=1}^{8} \frac{m_j}{i\omega_s - u_j} \quad , \quad (13)$$

and the poles $u_i$ and residues $m_i$ of $G^{at}_{ff,\sigma}(\omega_s)$ are all real (cf. Eq. (12)). There are only eight different $u_j$ for the f-electron GF, because different transitions have the same energy and the residues of some transitions are zero, and by analytic continuation one obtains $G^{at}_{ff,\sigma}(z)$, but there are more transitions for the $G^{at}_{cc,\sigma}(z)$.

The approximation employed in the present work consists in substituting $M^{eff}_{2,\sigma}(z)$ in Eq. (9) by the approximate $M^{at}_{2,\sigma}(z)$, derived from the exact $G^{at}_{ff,\sigma}(z)$ by solving for $M^{at}_{2,\sigma}(z)$ in the equation that is the atomic equivalent of Eq. (9). One then obtains

$$M^{at}_{2,\sigma}(z) = \frac{(z-E^a_0+\mu)\;\; G^{at}_{ff,\sigma}(z)}{\left(z-E^a_{0,\sigma}+\mu\right) - \mid V \mid^2 G^{at}_{ff,\sigma}(z)}, \quad (14)$$

and from the point of view of the cumulant expansion, it contains all the irreducible diagrams that contribute to the exact $M^{eff}_{2,\sigma}(\omega_s)$. It should be emphasized that this diagrams contain loops of any size, because there is no excluded site in this expansion, but all the local vertices correspond to the same site, although they appear as different vertices in each diagram. When a local hybridization is used (i.e. $V(\mathbf{k}) = V$), the only difference between the exact and approximate quantities is that different energies $E_{\mathbf{k},\sigma}$ appear in the c-electron propagators of the effective cumulant $M^{eff}_{2,\sigma}(\omega_s)$, while these energies are all equal to $E^a_{0,\sigma}$ in $M^{at}_{2,\sigma}(\omega_s)$. Although $M^{at}_{2,\sigma}(\omega_s)$ is for that reason only an approximation, it contains all the diagrams that should be present, and one would expect that the corresponding GF would have fairly realistic features.

One still has to decide what value of $E^a_{0,\sigma}$ should be taken. As the most important region of the conduction electrons is the Fermi energy, we shall use $E^a_{0,\sigma} = \mu - \delta E_0$, leaving the freedom of small changes $\delta E_0$ to adjust the results to particular situations, but fixing its value for a given system when $\mu$ has to change to keep the total number of electrons $N_t$ fixed, as for example when changing the temperature $T$.

Another important point, is that concentrating all the conduction electrons at $E^a_{0,\sigma}$ would overestimate their contribution to the effective cumulant, and we shall then reduce the hybridization by a coefficient that gives the fraction of c-electrons which contribute most. We consider that this is of the order of $V\varrho^0$, where $\varrho^0$ is the density of states of the free c electrons per site and per spin, and to be more definite we chose $\pi V\varrho^0$, so the effective hybridization constant $V_a$ coincides with the usual "mixing strength" $\Delta = \pi V^2\varrho^0$. This is essentially the same choice made by Alascio et.al.[27] in their localized description of valence fluctuations. Note that $V_a$ is only used in the calculation of $M^{at}_{2,\sigma}(z)$, and that the full value must be substituted in the $V$ that appears explicitly in Eq. (9), because the whole band of conduction energies is used in $G^o_{c,\sigma}(\vec{k},z) = -1/\left(z - \varepsilon_{\mathbf{k}\sigma}\right)$.

### B. Transport properties

Two particle GF should be used in the well known Kubo formula,[30,31] that relates the dynamic conductivity $\sigma(\omega,T)$ to the current current correlations. To simplify the calculations for the PAM, Schweitzer and Czycholl[29] employed the expression of the conductivity for dimension $d = \infty$ as an approximation of the static conductivity for $d = 3$. Only one-particle GFs are then necessary to obtain $\sigma(\omega,T)$ in that limit, because the vertex corrections cancel out,[33] and we shall use the same approximation. As the hybridization is a hopping of electrons between two different bands, it contributes to the current operator,[32] but this contribution cancels out in our model because we employ a local hybridization $V_{j,\mathbf{k},\sigma} = V_{j,\sigma}$. The expression obtained contains explicit sums over $\mathbf{k}$, but it is possible to make a further simplification by considering nearest-neighbor hopping in a simple cubic lattice,[34,35,36] and the sums over $\mathbf{k}$ can be transformed[37] in integrals over the free conduction electron energy $\varepsilon(\mathbf{k})$. This transformation is possible because in our method the $G_{cc,\sigma}(\mathbf{k},\omega)$ only depends on $\mathbf{k}$ through the $\varepsilon(\mathbf{k}) = \varepsilon$, as both $M^{at}_{2,\sigma}(z)$ and $V_{j,\mathbf{k},\sigma} = V_{j,\sigma}$ are $\mathbf{k}$ independent. We then obtain for the dynamic conductivity for each spin component

$$\sigma_\sigma(\omega,T) = C_0 \frac{1}{\omega}\int_{-\infty}^{\infty} d\omega\prime \left[f_T(\omega\prime) - f_T(\omega\prime+\omega)\right]\; L_\sigma(\omega,\omega') \tag{15}$$

where

$$L_\sigma(\omega,\omega') = \int_{-\infty}^{\infty} d\varepsilon\; \rho_{c,\sigma}(\omega\prime;\varepsilon)\; \rho_{c,\sigma}(\omega\prime+\omega;\varepsilon)\; \varrho^0_\sigma(\varepsilon), \tag{16}$$

$$\rho_{c,\sigma}(\omega;\varepsilon) = \frac{1}{\pi}\lim_{\eta\to 0}\; Im\left\{G_{cc,\sigma}(\mathbf{k},\omega + i\,|\eta|)\right\}, \tag{17}$$

and $f_T(\omega)$ is the Fermi function. The static conductivity for each spin component is then given by

$$\sigma_\sigma(T) = C_0\int_{-\infty}^{\infty} d\omega\; \left(-\frac{df_T(\omega)}{d\omega}\right)\; L_\sigma(\omega) \qquad , \tag{18}$$

where

$$L_\sigma(\omega) = \int_{-\infty}^{\infty} d\varepsilon\; \left(\rho_{c,\sigma}(\omega;\varepsilon)\right)^2\; \varrho^0_\sigma(\varepsilon) \qquad . \tag{19}$$

The constant

$$C_0 = \pi\;\frac{e^2}{\hbar}\;\frac{2}{a}\;\frac{2\;t^2}{d}, \tag{20}$$

where $a = 9.89\mathring{A}$ is the lattice parameter[4] of $Tl_2Mn_2O_7$, that has two sites per unit cell. We shall generally use a rectangular band with $-W \leqslant \varepsilon(\mathbf{k}) \leqslant W$, and we set $t = W/2d$ to estimate the hopping parameter $t$ of the hypercubic lattice, and use $d = 3$.

Employing reference [29] we obtain the expression for the thermopower $S(T)$ :

$$S(T) = \frac{\sum_\sigma \int_{-\infty}^{\infty} d\omega\;\omega\;\left(-\,df_T(\omega)/d\omega\right) L_\sigma(\omega)}{\sum_\sigma \int_{-\infty}^{\infty} d\omega\;\left(-\,df_T(\omega)/d\omega\right) L_\sigma(\omega)} \tag{21}$$

### C. The magnetization of the system

As the system consists of two independent subsystems (spin up and spin down) we could attribute arbitrary probabilities $P$ $(1-P)$ to the spin up (spin down) subsystem, and calculate the corresponding properties of the system. Following the work of Ventura and Alascio, we

shall estimate the probability $P$ from the system magnetization, that we calculated employing the Weiss molecular field approximation:

$$\frac{M}{M_{sat}} = \tanh\left\{\frac{\widetilde{\mu}\ B}{k_B\ T} + \frac{T_C\ M}{T\ M_{sat}}\right\}.$$

Here $\widetilde{\mu}$ is the local magnetic moment, $B$ the magnetic field, $T_C$ the Curie temperature and $M_{sat}$ the saturation magnetization. Following those authors we use $\widetilde{\mu} = 3\mu_B$, as intermediate between the 3.87 $\mu_B$ local moment of the $Mn^{5+}$ and the 2.83 $\mu_B$ corresponding to the $Mn^{4+}$.

To calculate the probability $P$ we then employ

$$M = [P - (1-P)]\ \widetilde{\mu},$$

and proceed to calculate the system properties as a function of $T$ for different values of the total number $n$ of electrons per site. Employing our approximate GF it is possible to calculate $n$ for each value of $P$ and $T$, and it is necessary to find the chemical potential $\mu$ that gives the required number of electrons per site.

## III. THE CALCULATION OF THE TRANSPORT PROPERTIES

We shall consider the stoichiometric $Tl_2Mn_2O_7$ compound, and we shall then fix the total number of electrons per site as $n = 1$. To keep this value constant, it might be necessary to change the chemical potential $\mu$ with the temperature $T$, and we shall employ the approximate GF $G^{at}_{ff,\sigma}(z)$ and $G^{at}_{cc,\sigma}(z)$ to calculate the number $n$ at each $T$ and then solve numerically the equation $n = 1$.

We shall use a rectangular band centered at the energy origin and with a half width $W = 6$ eV, and take the energies for the spin 1/2 and 1 in the presence of the field $B$ as $E_s = 2s\ \mu_B\ B$ and $E_\sigma = E^0_\sigma + \sigma\ 2\mu_B\ B$ , with $E^0_\sigma = -5.5$ eV, so that the spin 1/2 has the lowest energy of the local states at $B = 0$.

It seems clear that the basic scattering mechanism in our calculation of $\sigma\,(T)$ is the hybridization, because the otherwise free conduction electrons are scattered by the localized f electrons through this interaction. This is apparent if we notice that the relaxation effects are described by the imaginary part of the usual self-energy $\Sigma_{cc,\sigma}(\mathbf{k},z)$, defined through

$$G_{cc,\sigma}(\mathbf{k},z) = -\left\{z - \varepsilon(\mathbf{k}) - \Sigma_{cc,\sigma}(\mathbf{k},z)\right\}^{-1} \quad , \quad (22)$$

and that the exact relation $\Sigma_{cc,\sigma}(\mathbf{k},z) = -\ |\ V(\mathbf{k})\ |^2\ M^{eff}_{2,\sigma}(\mathbf{k},z)$ follows from Eq. (10). The relaxation mechanism of the c-electrons is then provided by the hybridization, and in our approximation the self energy $\Sigma_{cc,\sigma}(z) = -\ |\ V\ |^2\ M^{at}_{2,\sigma}(z)$ is independent of $\mathbf{k}$. It seems then clear that the resistivity at low temperatures depends sensitively on the value of $V$. This quantity also determines the position of the peak of the dynamic conductivity that is close to 2 e.V at 295 K, and to try and adjust the two different properties we have employed a temperature dependent hybridization $V$, using values that decrease from 2.5 eV to 1.8 eV as $T$ increases to 300 K.

We have also employed a value of $\Delta E_0 = E^a_0 - \mu$ that changes from $-1.2$ eV to $-0.9$ eV in the same temperature range, because it gives a better overall agreement with the experimental results.

To alleviate somehow the use of a zeroth width conduction band in the calculation of the effective cumulant we have added an extra imaginary part $\eta_a = 0.18$ eV to the complex variable $z$. Addition of $\eta_a$ to the argument of $M^{at}_{2,\sigma}(z)$ leads to similar effects as those already obtained by Mutou and Hirashima[34] through "introducing a small imaginary part $\Gamma$ to the conduction electrons", i.e. replacing $z = i\ \omega$ by $z + i\ \Gamma\ sgn(\omega)$ in the GFs $G_{ff,\sigma}(\mathbf{k},z)$ and $G_{cc,\sigma}(\mathbf{k},z)$. Their justification is the existence in real systems of scattering processes due to phonons and impurities, and we should also consider this mechanisms as contributing to the $i\eta_a$. Within this interpretation one could also consider a temperature dependence of $\eta_a$, but we have not implemented this change in the present calculation.

### A. The local spectral density of states

A very useful quantity is the local spectral density of the conduction electrons, namely

$$\rho_{c,\sigma}(\omega) = \frac{1}{\pi}\ \lim_{\eta\to 0}\ Im\left\{\frac{1}{N_s}\sum_{\mathbf{k}} G_{cc,\sigma}(\mathbf{k},\omega + i\ \ |\eta|)\right\} \quad (23)$$

because it illuminates the dependence with $T$ of the static conductivity. In figure 1 we plot $\rho_{c,\sigma}(\omega)$ at several temperatures above and below the critical temperature $T_C = 121$K, and for parameters that give a fair description of the properties we study.

At $T = 40$ K the $\rho_{c,\sigma}(\omega)$ is different for the two spin components. The magnetization is practically saturated and all the local spins point in the same direction, say up. The conduction electrons with spin up hybridize with the local spins, and in figure 1 is shown that a large gap is created with $\mu$ inside, so there is little conductivity by these electrons. As there are practically no local electrons with spin down, the conduction electrons do not have electrons to hybridize with, and there is no gap. The chemical potential $\mu$ is near near the bottom of the band, and the spin down electrons contribute strongly to the conductivity giving a vanishing resistivity as it is shown in figure 3.

At $T = 295$ K the probabilities of the two spin components at zero magnetic field are equal, and have the same spectral densities as shown in figure 1. The $\mu$ is inside a smaller gap, and the resistivity has increased, as shown in figure 3. For $T = 150$ K the $\rho_{c,\sigma}(\omega)$ has a larger gap but essentially the same features shown by the plot

at $T = 295$ K, although the hybridization and the $\Delta E_0$ employed here are practically the same used in the plot at $T = 40$ K.

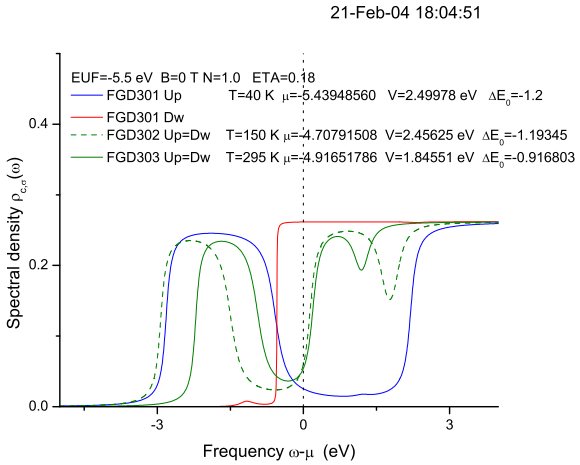


FIG. 1: The local spectral density of the conduction electrons $\rho_{c,\sigma}(\omega)$ at $T$ both below and above the critical temperature $T_C = 121$K, and for system parameters indicated in the figure. We employ a $T$ dependent $V$ and $\Delta E_0$, and their values together with $\mu$ are shown for each curve.

Integrating the spectral densities over $\omega$ we obtain the number of up ($n_{f,up}$) and down ($n_{f,dw}$) local electrons at each $T$, and we plot their values in figure 2. This sum of these two quantities gives the total number ($n_f$) of local electrons, and the plot shows that this quantity is fairly independent of $T$. The measurements of X ray absorption spectroscopy (XAS) in $Tl_2Mn_2O_7$[38] indicate that the Mn valence is fairly close to 4. Two facts point to the independence of this quantity with temperature. First, the XAFS indicates that the local structure coincides with the average one in $Tl_2Mn_2O_7$ and that there is no disorder in the same structures of this compound, differently from the disorder in the $MnO_6$ octahedra of the manganites, that is caused by Jahn-Teller distortions. Second, the Mn-O and Tl-O bonds in $Tl_2Mn_2O_7$ show normal Debye-like dependence, with no change in ordering at $T_c$, in contrast with the behavior of the $La_{0.75}Ca_{0.25}MnO_3$ manganite.[38]

Subramanian ed al.[39] conclude from the properties of $Tl_2Mn_2O_7$ that some of the $Mn^{4+}$ electrons go into the Tl band, so that the compound corresponds to $Tl^{3+}_{2-x}-Tl^{2+}_x Mn^{4+}_{2-x} Mn^{5+}_x O_7$, in agreement with the model of Ventura and Alascio.[12]

### B. The static resistivity and the magnetoresistance

We employ Eq. (18) to calculate the resistivity for each spin component, and we sum the two contributions to obtain the total conductivity. In figure 3 we plot the resulting resistivity as a function of $T$ for the following magnetic fields: $B = 0$ T, 2 T, 5 T, and 7 T, and the remaining system parameters are given in the figure. The values we calculated are of the same order of those reported by Shimakawa ed al.[15], and there is a sharp increase in the resistance at the critical temperature $T_C$; the increase becomes more gradual when the magnetic field increases. In figure 4 we plot quantities proportional to $\sigma_\sigma(T)$ for the up and down electrons at both $H = 0$ T and $H = 2$ T.

From the resistivity ad different magnetic fields we can calculate the negative magnetoresistance $(\rho(B = 0) - \rho(B))/\rho(B)$, plotted in figure 5. The value of the maximum near $T_C$ is close to that observed by Cheong ed al.[8], but the rise before the maximum is much steeper

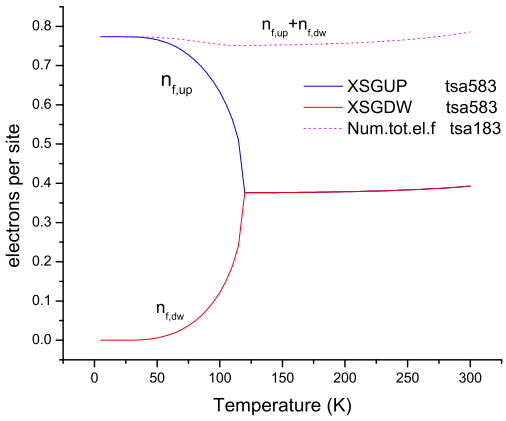


FIG. 2: The number of local electrons per site for spin up, spin down and for their sum, as a function of $T$. The system parameters are indicated in the figure.

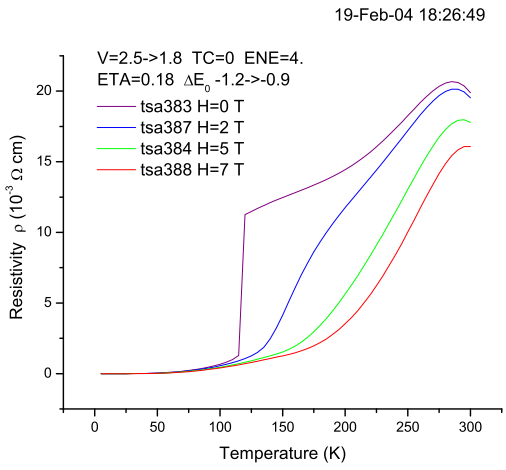


FIG. 3: The resistivity as a function of T for several magnetic fields, and for the system parameters indicated in the figure.

in our calculation.

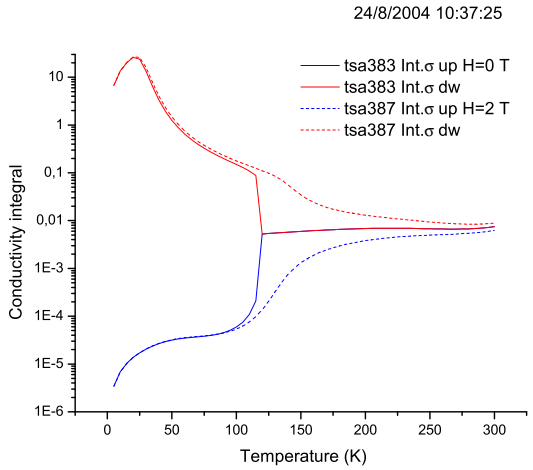


FIG. 4: Values proportional to $\sigma_\sigma(T)$ for up and down electrons at $H = 0$ T and $H = 2$ T.

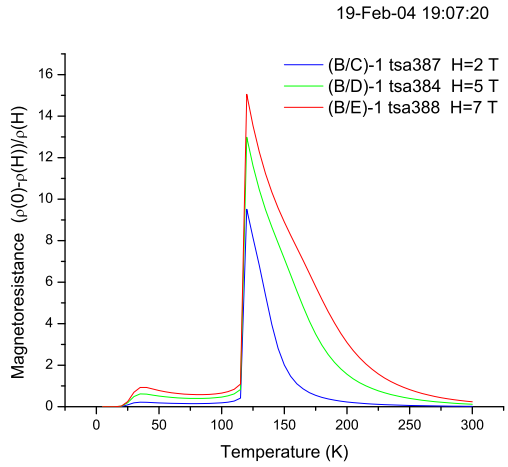


FIG. 5: The magnetoresistance as a function of T for several magnetic fields, and for system parameters indicated in the figure.

### C. The optical conductivity

We have employed Eq. (15) to calculate the optical conductivity $\sigma(\omega, T)$ as the sum of the contribution $\sigma_\sigma(\omega, T)$ of the two spin components. In the measurements of the optical conductivity of Okamura ed al.[14] one observes a strong peak close to $\omega = 2$ eV at $T = 295$ K. This type of measurement is expected to depend on the value of the direct gap, which is affected by the hybridization constant $V$. The static resistivity, on the other hand,

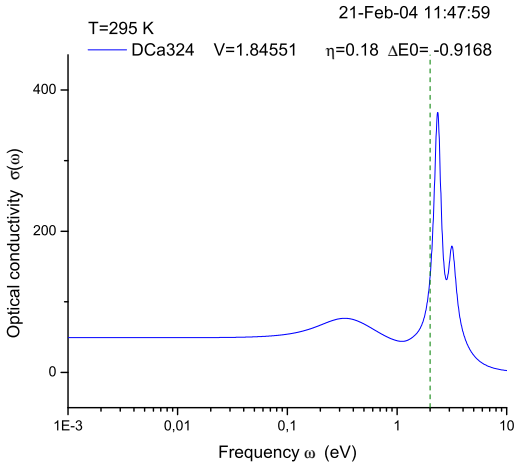


FIG. 6: The optical conductivity for system parameters indicated in the figure.

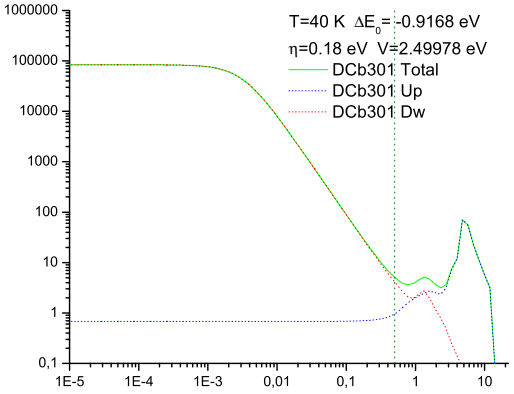


FIG. 7: Contribution of the two spin components to the optical conductivity at $T = 40$ K for system parameters indicated in the figure. The vertical line is located at 0.5 eV.

depends on the indirect gap, and the scattering mechanism at low temperatures depends also on the hybridization, as discussed before. We have then employed a temperature dependent value of $V$ to adjust these two quantities, and we used $V \simeq 1.85$eV at $T = 295$ K . In figure 6 we plot the the optical conductivity $\sigma(\omega, T)$ at $T = 295$ K, and we obtain a peak at the correct frequency. There are several smaller peaks at lower frequencies, that have been asigned to optical phonons.[14]

At low $T$ the two spin components make different contributions to $\sigma(\omega, T)$, as shown in figure 7. The component with spin down corresponds to a metal, and the corresponding $\sigma(\omega, T)$ describes the Drude peak of this metal, and the figure shows that the metallic components are limited to below 0.5 eV, as measured by Okamura ed al.[14]. Although the spectral density in figure 1 does not

give the direct gap, it is consistent with figure 7. The spin up component in figure 1 corresponds to a semiconductor, and in figure 7 it shows a very small $\sigma(\omega, T)$ at low frequencies, that starts to increase at $\omega \sim 3$ eV. The different contribution of the two spin components can also be understood by considering the sum rules[18,40,41] of the two spin components of $\sigma_\sigma(\omega, T)$ as two separate contributions, but we have not done a numerical analysis of this interpretation. The two components give identical contributions to $\sigma_\sigma(\omega, T)$ above $T_C$, because the two bands are identical when the magnetization becomes zero.

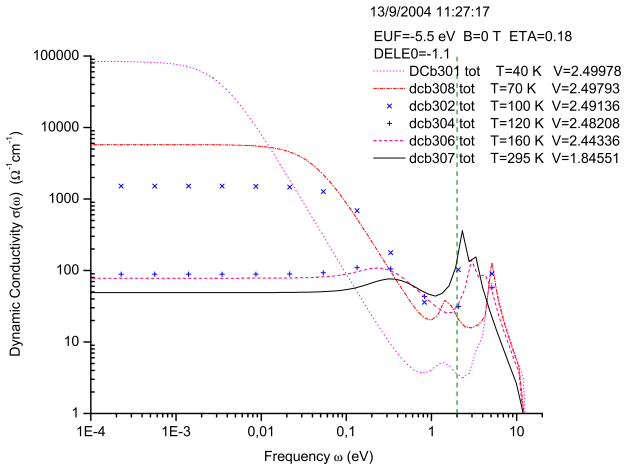


FIG. 8: The optical conductivity at low frequencies for several temperatures.The values of $\sigma(\omega, T)$ when $\omega \to 0$ give the temperature dependence of the Drude peak

In figure 8 we plot the optical conductivity for several temperatures. At low frequencies one can see how the maximum of the Drude peak at $\omega = 0$ decreases and its width increases when $T$ increases.

### D. The thermopower and the magneto thermopower

We have employed Eq. (21) to calculate the thermopower $S(H, T)$ of $Tl_2Mn_2O_7$ within the model of Ventura and Alascio, and in figure 9 we show the temperature dependence for several magnetic fields. The plot agrees qualitatively with the experimental results of Imai ed al.[9] and at $H = 0$ T it is approximately linear in $T$ just below and above $T_C$ , but with different slopes. We employed Eq. (21) to calculate $S(H, T)$, because the model is composed of two independent subsystems. It is then straightforward to calculate the magneto-thermopower, defined by $\Delta S(H) = S(H) - S(0)$, and in figure 10 we plot our results, that show a semi quantitative agreement with those in reference 9: the magnitude of $\Delta S(H)$ is of the same order, but the increase at $T_C$ is more abrupt than the one measured experimentally.

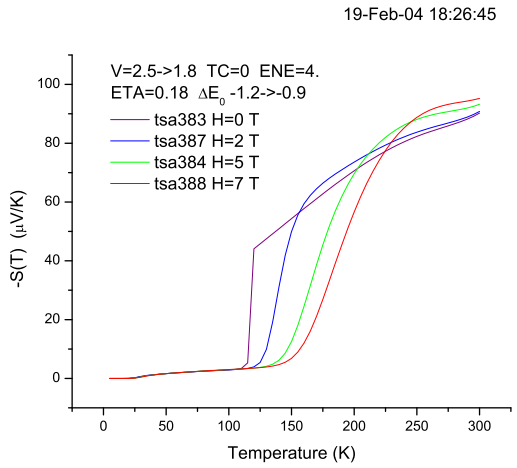


FIG. 9: The thermopower for system parameters indicated in the figure.

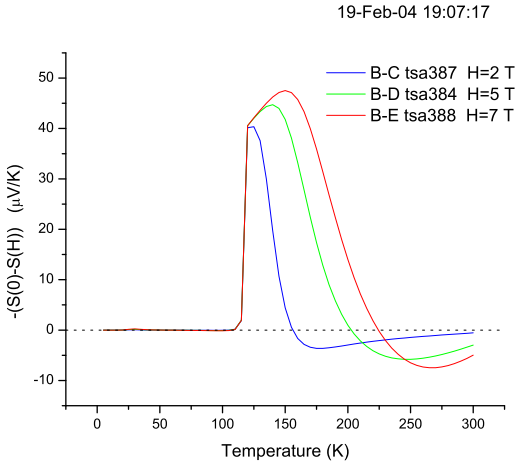


FIG. 10: The magneto thermopower for system parameters indicated in the figure.

## IV. CONCLUSIONS

Asuming that the system is stoichiometric we have calculated the resistivity, optical conductivity and thermopower as a function of temperature and magnetic field of the model of $Tl_2Mn_2O_7$ introduced by Ventura and Alascio.[12] Differently from other studies, we have calculated these transport properties employing Kubo's formula, that is directly related to the electronic GFs. To derive these GFs we introduced Hubbard operators to describe the model, and used a treatment previously employed to study FeSi.[13,18] With the dependence of resistivity and thermopower with magnetic field we have also calculated the magneto resistance and the magneto thermopower.

We obtain a semiquantitative agreement with the experimental results by an adequate choice of the system parameters, and we can conclude that the model gives a fair description of all the calculated properties.

### Acknowledgments

The authors would like to acknowledge financial support from the following agencies: FAPESP and CNPq. They are grateful to B. R. Alascio and C. Ventura for suggesting this study and for several interesting discussions.

## APPENDIX A: ATOMIC EIGENSTATES

In table I we give the atomic eigenstates $\mid j,\nu,r\rangle$ of $H_j$ (cf. Eq. (11)) as a function of the eigenstates for $V=0$. To abbreviate we use $E_\pm = E_{\pm 1/2}$, $\varepsilon_\pm = E_{\pm 1} - \mu$, $\varepsilon^0_\pm = E^a_{0,\pm} - \mu$, and $\varepsilon^0_2 = \varepsilon^0_+ + \varepsilon^0_-$ as well as the following energy expressions that appear often in the formulas

$$\varepsilon_{m\pm} = \left(\varepsilon_\pm - E_\pm - \varepsilon^0_\pm\right)/2$$
$$\varepsilon_{s\pm} = \left(\varepsilon_\pm + E_\pm + \varepsilon^0_\pm\right)/2$$
$$r_\pm = \sqrt{\left(\varepsilon_{m\pm}\right)^2 + |V|^2}$$

The coefficients of the eigenfunctions in table I are obtained from

$$tg\phi_\pm = \pm tg\ \psi_\pm = \frac{V^*}{\varepsilon_{m\pm} + r_\pm},$$

and we conventionally use $\cos\phi_\pm > 0$ and $\cos\psi_\pm > 0$ to specify the sign of the eigenfunctions.

| $\mid n,r\rangle$ | Eigenstate | $S_z$ | $\varepsilon_r = E_r - n_r\mu$ |
|---|---|---|---|
| $\mid 0,1\rangle$ | $\mid -\frac{1}{2},0\rangle$ | $-1/2$ | $\varepsilon_1 = E_-$ |
| $\mid 0,2\rangle$ | $\mid +\frac{1}{2},0\rangle$ | $+1/2$ | $\varepsilon_2 = E_+$ |
| $\mid 1,3\rangle$ | $C\phi_- \mid -1,0\rangle - S\phi_- \mid -\frac{1}{2},\downarrow\rangle$ | $-1$ | $\varepsilon_3 = \varepsilon_{s-} + r_-$ |
| $\mid 1,4\rangle$ | $C\phi_+ \mid +1,0\rangle - S\phi_+ \mid +\frac{1}{2},\uparrow\rangle$ | $+1$ | $\varepsilon_4 = \varepsilon_{s+} + r_+$ |
| $\mid 1,5\rangle$ | $S\phi_- \mid -1,0\rangle + C\phi_- \mid -\frac{1}{2},\downarrow\rangle$ | $-1$ | $\varepsilon_5 = \varepsilon_{s-} - r_-$ |
| $\mid 1,6\rangle$ | $S\phi_+ \mid +1,0\rangle + C\phi_+ \mid +\frac{1}{2},\uparrow\rangle$ | $+1$ | $\varepsilon_6 = \varepsilon_{s+} - r_+$ |
| $\mid 1,7\rangle$ | $\mid -\frac{1}{2},\uparrow\rangle$ | $0$ | $\varepsilon_7 = E_- + \varepsilon^0_+$ |
| $\mid 1,8\rangle$ | $\mid +\frac{1}{2},\downarrow\rangle$ | $0$ | $\varepsilon_8 = E_+ + \varepsilon^0_-$ |
| $\mid 2,9\rangle$ | $\mid -1,\downarrow\rangle$ | $-3/2$ | $\varepsilon_9 = \varepsilon_- + \varepsilon^0_-$ |
| $\mid 2,10\rangle$ | $\mid +1,\uparrow\rangle$ | $+3/2$ | $\varepsilon_{10} = \varepsilon_+ + \varepsilon^0_+$ |
| $\mid 2,11\rangle$ | $C\psi_- \mid -1,\uparrow\rangle - S\psi_- \mid -\frac{1}{2},\uparrow\downarrow\rangle$ | $-1/2$ | $\varepsilon_{11} = \varepsilon_3 + \varepsilon^0_+$ |
| $\mid 2,12\rangle$ | $C\psi_+ \mid +1,\downarrow\rangle - S\psi_+ \mid +\frac{1}{2},\uparrow\downarrow\rangle$ | $+1/2$ | $\varepsilon_{12} = \varepsilon_4 + \varepsilon^0_-$ |
| $\mid 2,13\rangle$ | $S\psi_- \mid -1,\uparrow\rangle + C\psi_- \mid -\frac{1}{2},\uparrow\downarrow\rangle$ | $-1/2$ | $\varepsilon_{13} = \varepsilon_5 + \varepsilon^0_+$ |
| $\mid 2,14\rangle$ | $S\psi_+ \mid +1,\downarrow\rangle + C\psi_+ \mid +\frac{1}{2},\uparrow\downarrow\rangle$ | $+1/2$ | $\varepsilon_{14} = \varepsilon_6 + \varepsilon^0_-$ |
| $\mid 3,15\rangle$ | $\mid -1,\uparrow\downarrow\rangle$ | $-1$ | $\varepsilon_{15} = \varepsilon_- + \varepsilon^0_2$ |
| $\mid 3,16\rangle$ | $\mid +1,\uparrow\downarrow\rangle$ | $+1$ | $\varepsilon_{16} = \varepsilon_+ + \varepsilon^0_2$ |

TABLE I: The sixteen eigenstates $\mid n,r\rangle$ of $\mathcal{H}$ are given as a function of the eigenstates in the absence of hybridization, together with their eigenvalues $\varepsilon_{n,r} = E_{n,r} - n\mu$, where $E_{n,r}$ is the energy of the state $\mid n,r\rangle$. To abbreviate we used $C\phi_\pm$ =cos$\phi_\pm$, $S\phi_\pm$ =sen$\phi_\pm$, $C\psi_\pm$ =cos$\psi_\pm$ and $S\psi_\pm$ =sen$\psi_\pm$.


[1] D.J. Singh, *Phys. Rev.* **B** 55, 313, (1997)
[2] A.P. Ramirez and M.A. Subramanian, *Science* **277**, 546 (1997)
[3] S.K Mishra and S. Satpathy *Phys. Rev.* **B** 58, 7585, (1998)
[4] Y. Shimakawa,Y. Kubo, N. Hamada, D. Jorgensen, Z. Hu, S. Short, M. Nohara and H. Takagi, *Phys. Rev.* **B** 59, 1249, (1999)
[5] N.P. Raju, J.E. Greedan and M. A. Subramanian *Phys. Rev.* **B 49**, 1086 (1994)
[6] Y. Shimakawa, Y. Kubo and T. Manako, *Nature* **379**, 53 (1996)
[7] B.Martínez, R. Senis, J. Fontcuberta, X. Obradors, W. Cheikh-rouhou, P. Strobel, C. Bougerol-Chaillout and M. Pernet, *Phys. Rev. Lett.,* **83**, 2022 (1999)
[8] S-W Cheong, H. Y. Wang, B Bstlogg, L.W. Rupp, *Sol. State Comm.*, **98,** 163 (1996)
[9] H. Imai, Y. Shimakawa, Yu. V. Shusko and Y Kubo *Phys. Rev.* **B** 62, 12190, (2000)
[10] Yu. V. Sushko, Y. Kubo, Y. Shimakawa and T. Manako *Physica* **B 259-261, 831** (1999)
[11] M.D. Nuñez-Regueiro and C. Lacroix *Phys. Rev.* **B 63**, 014417 (2000)
[12] C. Ventura and B. Alascio, *Phys. Rev.* **B** 56, 14533 (1997)
[13] M.E. Foglio and M. Figueira, *Phys. Rev.* **B** 60, 11361, (1999)
[14] H. Okamura, T. Koretsune, M. Matsunami, S Kimura, T, Namba, H. Imai, Y Shimakawa and Y. Kubo *Phys. Rev.* **B** 64, 180409 (2001)
[15] Y. Shimakawa, Y. Kubo, N. Hamada, J. D. Jorgensen, Z. Hu, S. Short, N. Nohara, and H. Takagi *Phys.Rev.* **B** 55, 6399, (1997)
[16] H. Schweitzer and G. Czycholl *Phys. Rev.Letters* **67**, 3724 (1991)
[17] N. Furukawa, *J. Phys. Soc. Japan* **63**, 3214 (1994).
[18] M.E. Foglio and M. Figueira, *Phys. Rev.* **B** 62, 7882, (2000)
[19] A. L. Fetter and J. D. Walecka, Quantum Theory of Many-Particle Systems (McGraw-Hill, New York, 1971).
[20] J. Hubbard, Proc. R. Soc. London, Ser. A 296, 82 (1966)
[21] M. S. Figueira, M. E. Foglio and G. G. Martinez, Phys. Rev. B 50, 17933 (1994)
[22] W. Metzner, Phys. Rev. B 43, 8549 (1991)
[23] P. Fulde, *Solid State Physics* **41**, 1 (1988)See Appendix A
[24] A. C. Hewson, *The Kondo problem to Heavy Fermions*(Cambridge U.P. Cambridge, 1993)
[25] J. W. Negele and H. Orland *Quantum Many-Particle Systems* (Addison-Wesley, New York, 1988), Chap. 2.

[26] D. N. Zubarev, Usp. Fiz. Nauk. **71**, 71 (1960) [Sov. Phys.-Usp. **3**, 320 (1960)]
[27] B. Alascio, R. Allub and A. A. Aligia, Z. Phys. B **36,** 37 (1979)
[28] G. G. Martinez Pino, *Doctoral Thesis* (Campinas, SP, Brasil: Universidade Estadual de Campinas, 1989).
[29] H. Schweitzer and G. Czycholl *Phys. Rev. Letters*, **67**, 3724 (1991)
[30] R. Kubo, J. Phys. Soc. Japan **12,** 570 (1957)
[31] G. D. Mahan *Many-Particle Physics* (Plenum Press, New York, 1990).
[32] G. Czycholl and H. J. Leder, Z. Phys. B **44,** 59 (1981)
[33] A. Khurana, Phys. Rev. Lett. **64**, 1990 (1990)
[34] T, Mutou and D. S. Hirashima, J. Phys. Soc. Japan **63**, 4475 (1994)
[35] Th. Pruschke, D. L. Cox and M. Jarrell, Phys. Rev. B **47**, 3553 (1993)
[36] R. Consiglio and M. A. Gusmão, Phys. Rev. B **55**, 6825 (1997)
[37] E. Muller Hartmann, Z. Phys. B **74**, 507 (1989)
[38] G. H. Kwei, C. H. Booth, F. Bridges, M. A. Subramanian, Phys. Rev. B **55**, R688 (1997)
[39] M. A. Subramanian, B. H. Toby, A. P. Ramirez, W. J. Marshall, A. W. Sleight, G. H. Kwei, Science **273**, 81 (1996)
[40] M. J. Rozenberg, G. Kotliar and H. Kajueter, Phys. Rev. B **54**, 8452 (1996)
[41] D. Baeriswyl, C. Gros and T. M. Rice, Phys. Rev. B **35**, 8931 (1987)